

The Longitudinal Dynamic Behaviour of Sailplanes as Affected by Mass Balancing of the Control System

Pierluigi Duranti, Politecnico di Torino

Presented at the XVth OSTIV Congress, Räkälä, Finland (1976)

Abstract

A rational investigation is developed towards the clarification of the main effects which the masses set along the control system, their position, their arms and gear ratios can produce on the dynamic stability "stick free" of a sailplane in the particular case of "all moving tail", with the hinge line on the aerodynamic centre and without geared tab. In fact, this very situation is considered the worst as far as pilot induced oscillations are concerned, due to the high natural frequency of the free elevator which comes from a zero gradient $\partial c_{\mu} / \partial \delta$ of the aerodynamic hinge moment and from a light spring stiffness.

In combining the above variables, three significant dimensionless parameters have been defined, all three being directly connected to the inertial coupling between the sailplane and its control system.

On the basis of computer calculations, which refer to the M 300 prototype, the direct dependence of the short period frequency and damping on the above parameters is pointed out. General indications are then derived in order to fulfil the pilot's request for an adequate stick force per "g" gradient and, at the same time, to prevent undamped (or insufficiently damped) longitudinal short period oscillations.

Introduction

The idea of undertaking this study originated from observations made by Piero Morelli whilst piloting the prototype M 300 during the first flight tests. In fact, the sailplane performed undamped longitudinal short period oscillations "stick-free" (period of the order of 1 sec.) which the pilot was unable to stop; in

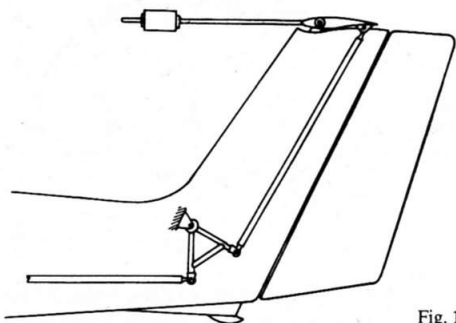


Fig. 1

fact his action had opposite effects revealing a species of "pilot induced oscillation". A solution was found by connecting a suitable balancing mass to the elevator (in this case an all moving tail - see fig. 1).

The best mass position, with respect to the elevator hinge line, was experimentally determined on the basis of a series of flight tests. Subsequently the mass, with its arm, was set inside the sailplane fuselage (fig. 2).

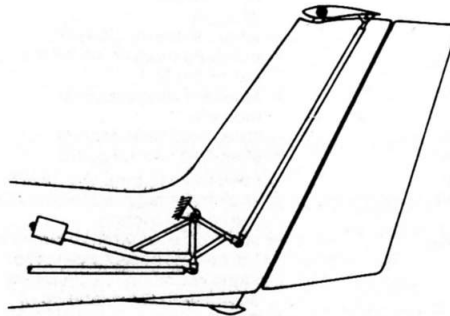


Fig. 2

The inertial coupling between the longitudinal control system and the sailplane itself appeared to be the main cause of the oscillation phenomenon. It was thought that a theoretical analysis of the dynamic stability of a sailplane control-free, with particular attention to the control system parameters, would shed light upon the causes of the undesirable motion, and so indicate how to prevent it in design.

Theoretical Background

In order to describe the longitudinal motion of the system sailplane control system in the case of "stick free", the following four differential equations were written; as generally involved in control-free stability problems, they express the dynamic equilibrium of the system with reference to each of the four degrees of freedom which were considered: forward displacement (through its time derivative V), angle of attack (α), angle of pitch (ϑ) and elevator deflection (δ).

$$(1) \quad \begin{aligned} F_x &= m\dot{V} \\ F_z &= -mV\dot{\gamma} = -mV(\dot{\vartheta} - \dot{\alpha}) \\ M_y &= J_y \ddot{\vartheta} \\ M_h &= J_{h\delta} \ddot{\delta} + J_{h\vartheta} \ddot{\vartheta} - S_{Mt} V(\dot{\vartheta} - \dot{\alpha}) \end{aligned}$$

With reference to the sketch in fig. 3:

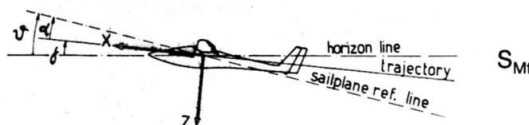


Fig. 3

F_x and F_z are the components of the external force, acting on the sailplane, along the eulerian "wind axes" x and z .

M_y is the resultant moment of the external forces with respect to the pitching axis y (normal to the xz plane).

M_h is the resultant moment of the external aerodynamic and spring forces acting on the whole control system and on the elevator, transferred to the elevator hinge line.

J_y is the inertia moment of the whole sailplane with respect to the y axis.

$J_{h\delta}$ is the inertia moment, sum of the contribution of the elevator (J_e), of the n concentrated masses, if any,

$$\sum_{i=1}^n m_i b_i^2 k_i^2$$

and of the equivalent inertia moment (J_{eq}) of the control system transferred to the elevator hinge line.

is a particular parameter, with the dimensions of an inertia moment, which should be regarded with the utmost attention, being the cause of the angular coupling between the sailplane and its control system; it is, in fact, a sort of mixed inertia moment which, multiplied by the sailplane angular acceleration $\ddot{\vartheta}$, gives a moment which affects the dynamic equilibrium of the elevator. It should be noticed that this "mixed moment" may be either positive or negative according to the mass distribution along the control system. From the expression

$$J_{h\delta} = \sum_{i=1}^n k_i m_i b_i (l_i + b_i) + J_e$$

and according to the scheme in fig. 4 one can, in fact, see that the distances l_i and b_i are considered positive when measured backwards from the sailplane centre of gravity and from the hinge, respectively. (When the value of $J_{h\delta}$ is zero, there is no angular coupling between the sailplane motion and that of the elevator).

S_{Mt} is the equivalent static moment of the elevator and control system, transferred to the hinge line of the elevator.

$$S_{Mt} = \sum_{i=1}^n m_i b_i k_i + S_{Me}$$

where S_{Me} is the elevator static moment with respect to the hinge line.

For the other symbols, see the list at the end.

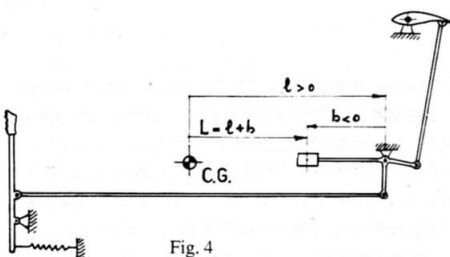
Method of Analysis

As in most cases of mathematical models of physical phenomena, a few simplifying hypotheses were introduced into this study. As one can see in equations [1], the unavoidable friction forces on the control system are not taken into account. In fact, the difficulty of correctly solving differential equations where friction effects are introduced is well known. In this first approach to the problem it was thought that results, obtained under this assumption, could be acceptable as indicative. In a subsequent investigation it will be possible to introduce friction effects and overcome the difficulty by digital simulations of the system motion.

The following fundamental hypotheses, commonly accepted, were then introduced:

- External forces and moments depend only on the variables $V, \alpha, \vartheta, \delta$ and on their first time derivatives.
- The motions herein considered consist of small disturbances of the variables around the initial conditions of trimmed flights.

On the basis of these hypotheses it becomes easier to deal with the above equations. The first three equations were developed as commonly explained in the classical literature (see ref. 1, 2, 3): the lengthy derivations of the dimensionless and linearised expressions [4] are then omitted. On the contrary, several passages, which refer to the fourth equation, have been emphasized; it is, in fact, the most interesting as it displays the three significant parameters which represent the object of this study. On the basis of the above considerations and with reference to fig. 4, which illustrates a typical control system for an



all-moving tail, the equilibrium equation around the elevator hinge line may be written as:

$$[2] \Delta M_h = -K_{\ell, trim} \Delta \delta + \frac{1}{2} \rho V^2 S_e \ell_e (C_{\mu} \dot{\vartheta} - C_{\mu} \delta) + \frac{1}{2} \rho S_e \ell_e C_{\mu} (V_t^2 - V^2) = \int_{h\delta} \ddot{\delta} + \int_{h\dot{\vartheta}} \ddot{\vartheta} - S_{Mt} V (\dot{\vartheta} - \dot{\alpha})$$

Dividing by $\frac{1}{2} \rho V_t^2 S_e \ell_e$ and introducing the following expressions:

$$[3] P_t = \frac{2 \rho S^2}{(Q/\rho)^2 S_e \ell_e} \cdot J_{h\delta} \quad P_{bob} = \frac{2 \rho S^2}{(Q/\rho)^2 S_e \ell_e} \cdot J_{h\dot{\vartheta}} \\ S_t = \frac{S}{(Q/\rho) S_e \ell_e} S_{Mt} \quad K = \frac{2 K_{\ell, trim}}{\rho S_e \ell_e V_t^2} \\ h_t = \frac{2 \rho S J_y}{(Q/\rho)^2 \ell_m} \quad V_t \cong V$$

the dimensionless form of the equation can be obtained. By operating in the same way on the first three equations, the ordered system is finally obtained:

$$[4] \begin{cases} (C_D + \frac{d}{d\tau}) \frac{\Delta V}{V_t} + \frac{1}{2} (C_{D\alpha} - C_L) \Delta \alpha + \frac{C_L}{2} \Delta \vartheta = 0 \\ C_L \frac{\Delta V}{V_t} + (C_{L\alpha} + \frac{d}{d\tau}) \Delta \alpha - \frac{d}{d\tau} \Delta \vartheta = 0 \\ (C_{M\alpha} + C_{M\alpha} \frac{d}{d\tau}) \Delta \alpha + (C_{M\vartheta} \frac{d}{d\tau} - h \frac{d^2}{d\tau^2}) \Delta \vartheta + (C_{M\delta} + C_{M\delta} \frac{d}{d\tau}) \Delta \delta = 0 \\ 2 S \frac{d}{d\tau} \Delta \alpha + [P_{bob} \frac{d^2}{d\tau^2} - (2 S_e + C_{\mu} \frac{d}{d\tau}) \frac{d}{d\tau}] \Delta \vartheta + [P_t \frac{d^2}{d\tau^2} - C_{\mu} \frac{d}{d\tau} - h] \Delta \delta = 0 \end{cases}$$

One should note that the comma ($\dot{\alpha}$ etc.) means differentiation with respect to the dimensionless "aerodynamic time" $\tau = t \cdot S \cdot V_t \cdot \rho / m$ so that, for instance, the following expressions are valid:

$$C_{M\alpha} \dot{\vartheta} = C_{M\alpha} \dot{\vartheta} \Rightarrow C_{M\alpha} = C_{M\alpha} \frac{\dot{\vartheta}}{\vartheta} = C_{M\alpha} \frac{d\vartheta}{d\tau} \frac{d\tau}{dt} = C_{M\alpha} \frac{\rho S V_t}{m}$$

It is then clear that results will refer to this particular time. The foregoing system must be satisfied, at each instant of the motion, by solutions in the form of:

$$\Delta \alpha = \Delta \alpha_0 e^{\lambda \tau} \quad \Delta \vartheta = \Delta \vartheta_0 e^{\lambda \tau} \\ \Delta \delta = \Delta \delta_0 e^{\lambda \tau} \quad \frac{\Delta V}{V_t} = \frac{\Delta V_0}{V_t} e^{\lambda \tau}$$

By substituting in [4] and simplifying, a system of algebraic equations is obtained in the variables $\Delta \alpha_0, \Delta \vartheta_0, \Delta \delta_0, \frac{\Delta V_0}{V_t}$

The features of the motions will be indicated by the nature of the complex roots of the usual "characteristic equation", obtained by expanding and setting to zero the following determinant:

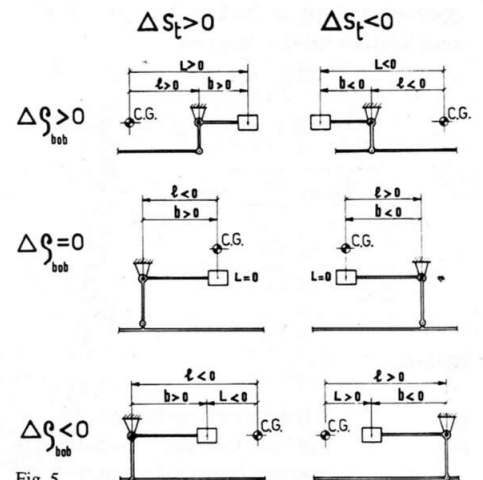
$$[5] \begin{vmatrix} C_D + \lambda \frac{1}{2} (C_{D\alpha} - C_L) & \frac{C_L}{2} & 0 \\ C_L & \frac{C_{L\alpha} + \lambda}{2} & -\lambda \\ 0 & C_{M\alpha} + C_{M\alpha} \lambda & C_{M\vartheta} \lambda - h \lambda^2 & C_{M\delta} + C_{M\delta} \lambda \\ 0 & 2 S \lambda & P_{bob} \lambda^2 - (2 S_e + C_{\mu} \lambda) & P_t \lambda^2 - C_{\mu} \lambda + h \end{vmatrix}$$

The characteristic equation, in the general case of stick-free, is a polynomial of the sixth degree, of the form:

$$[6] P_6 \lambda^6 + P_5 \lambda^5 + P_4 \lambda^4 + P_3 \lambda^3 + P_2 \lambda^2 + P_1 \lambda + P_0 = 0$$

where the coefficients P_i depend upon the aerodynamic, elastic and inertial parameters of the system.

At this point, a brief digression may be useful to clarify more significantly, the true meaning of the parameters Q_t, Q_{bob}, S_t . Fig. 5 gives a pictorial



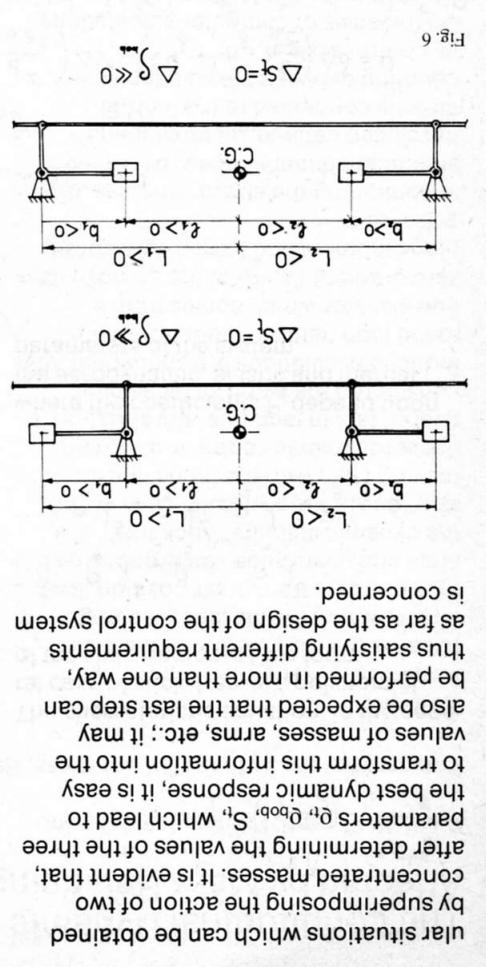
representation of the connection between the variables m_i, k_i, b_i, L_i and the consequent variation which they cause, ΔS_t and ΔQ_{bob} . It should be remarked that, in this scheme, only one mass is indicated. It is, however, possible to superimpose the different situations in order to obtain the desired effect. In fact fig. 6 shows, for instance, two partic-

ular situations which can be obtained by superimposing the action of two concentrated masses. It is evident that, after determining the values of the three parameters ζ and ω_n , which lead to the best dynamic response, it is easy to transform this information into the values of masses, arms, etc.; it may also be expected that the last step can be performed in more than one way, thus satisfying different requirements as far as the design of the control system is concerned.

The procedure described was followed by running a Fortran program developed for this goal. For each combination obtained by varying the above parameters, the program expands the determinant of coefficients (5) and, subsequently, solves the resultant characteristic equation (6). From the six complex roots so obtained, the program easily computes the features of the corresponding motions of the sailplane control system. In fact the following well known relations exist:

$$\lambda = a + i b = \zeta \omega_n \pm i \omega_d$$

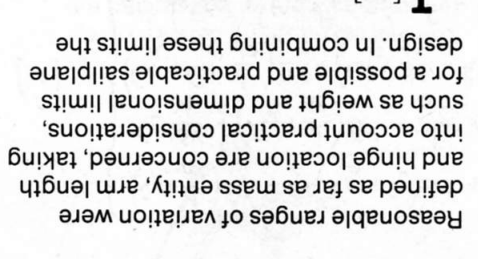
$$\zeta_{double} = \frac{2\omega_d}{\omega_n} \text{ or } \zeta_{half} = \frac{\omega_d}{\omega_n}$$



As our characteristic equation is dimensionless, it must be noticed that these relations refer to aerodynamic time. If actual values are desired, they must be corrected with respect to real time. As mentioned above, the calculations of the present study were made with reference to the M 300 prototype, designed by Alberto and Piero Morelli of the Politecnico of Turin. A three view drawing of the M 300 is shown in fig. 7.

$$-0.05 \leq \zeta \leq 0.06 \text{ and } 0.008 \leq \zeta \leq 0.025$$

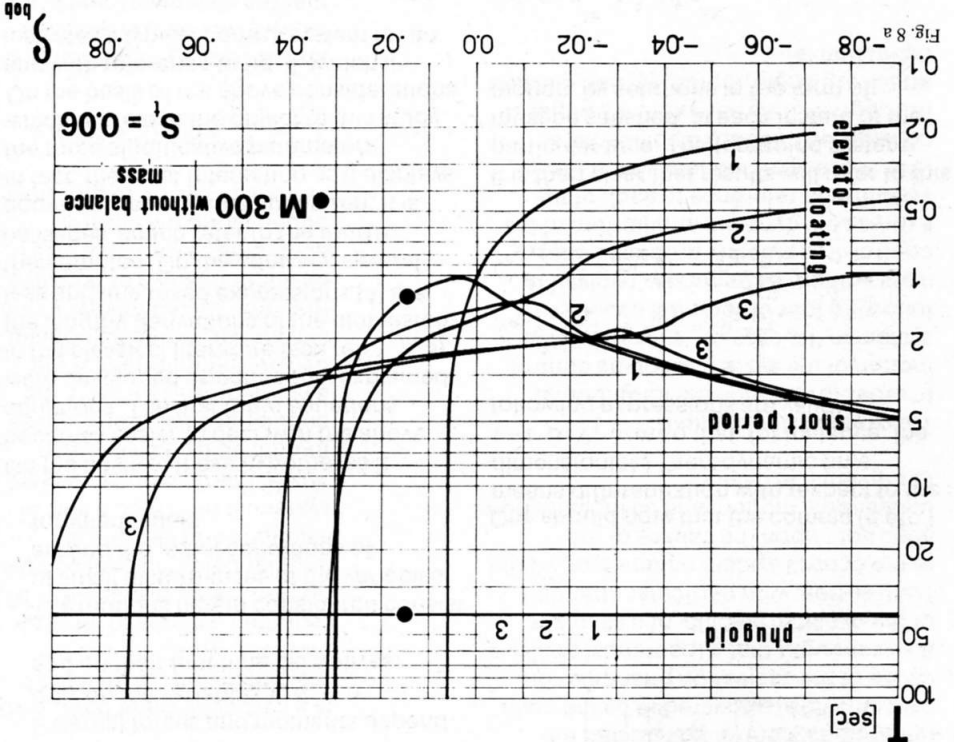
Reasonable ranges of variation were defined as far as mass entity, arm length and hinge location are concerned, taking into account practical considerations, such as weight and dimensional limits for a possible and practicable sailplane design. In combining these limits the abscissa ζ_{pop} is indicated. The ordinate scale (seconds) takes three logarithmic decades, from 0.1 to 1 sec., from 1 to 100 [sec].



As expected, solving the characteristic equation leads, in the most general case, to three pairs of complex roots; it is well known that the fairly distinct modes of oscillation which refer to each of them are: the phugoid, the short period and a third mode which is identified by the free oscillation of the elevator around its hinge line. In particular cases, one or more of these modes degenerates into exponential form. Fig. 8a shows on the same diagram, in semi-logarithmic scale, the period of oscillation of the three modes. It refers to a well defined value of S_1 , or, in other words, to a well defined value of the stick-force per "g" contribution. In fact it is just this parameter which determines the amount of the contribution given to the stick force per "g" gradient by the control system, according to the following relation:

$$\left[\frac{C_n}{C_p} \right]_{bob} = -\sigma \cdot g \cdot \frac{S_1}{z} \left[\frac{C_n}{C_p} \right]_{stick}$$

Analysis of results



As one can see three families of curves are plotted, marked 1, 2, 3, respectively. They refer to three different values of ζ , 0.0008, 0.005, 0.025, respectively, corresponding to approximately minimum, medium and maximum values of the inertia moment of the whole control system around the elevator hinge line.

Fig. 8a

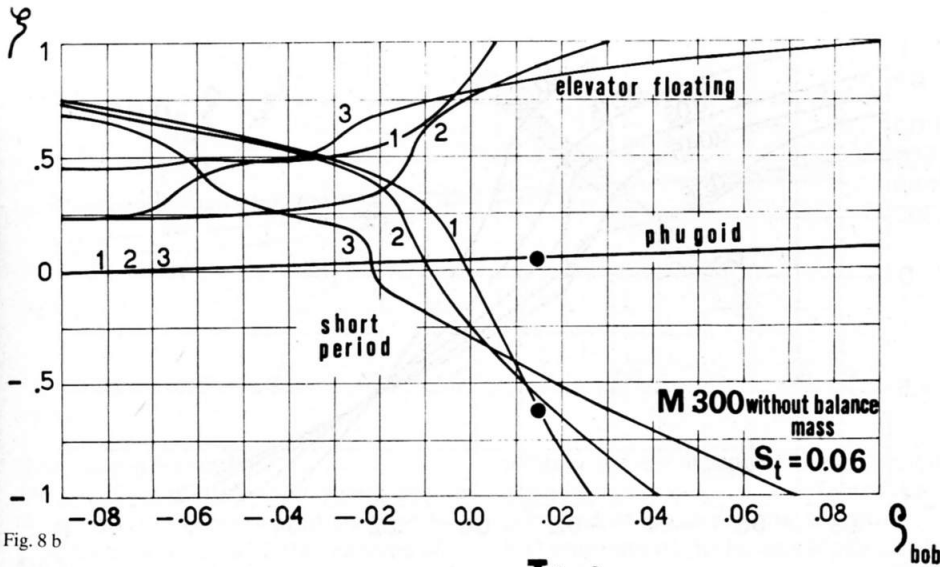


Fig. 8b

Fig. 8b refers to the diagram of the damping coefficient, which corresponds to the above curves of period of oscillation. By analysing figs. 8a and 8b, one can see that the curves 1, 2, and 3, as far as the long period is concerned, are coincident in period and damping; they are not affected by the variation of q_t . This could have been expected, as the natural frequency of the free elevator is very high if compared with the low frequency of the phugoid mode where the floating elevator mode is completely filtered and cannot affect the sailplane's long period features. On the contrary, as one can see, the influence of q_t on the features of the elevator floating appears to be very high; together with the trim spring stiffness, it directly affects the natural frequency of the control system. This effect is reflected in the short period behaviour, on which the effect of Q_{bob} is appreciable.

The most noticeable and important effect is in fact that of the variations of Q_{bob} on the short period mode. For appreciably negative values of this parameter the three modes appear to be very distinct: one can see a phugoid with a period of approximately 40 secs., neutrally damped, a short period heavily damped ($=0.7-0.75$) for all three values of q_t , and the fast oscillation of the elevator (period varying from 0.2 to 2 secs.), according to the values of q_t , with a damping which varies from 0.25 to 0.45.

For increasing Q_{bob} one can see that, whilst the phugoid mode is only slightly affected in the sense of increasing its damping, the short period shows a rapid reduction in damping and in its period of oscillation, which approaches the thresholds of 1, 1.5, 1.8 secs., respectively. These are considered dangerous limits, particularly in the presence of very low damping, as they are associated with a strong possibility that pilot induced oscillations will occur. The curves of period show minima cor-

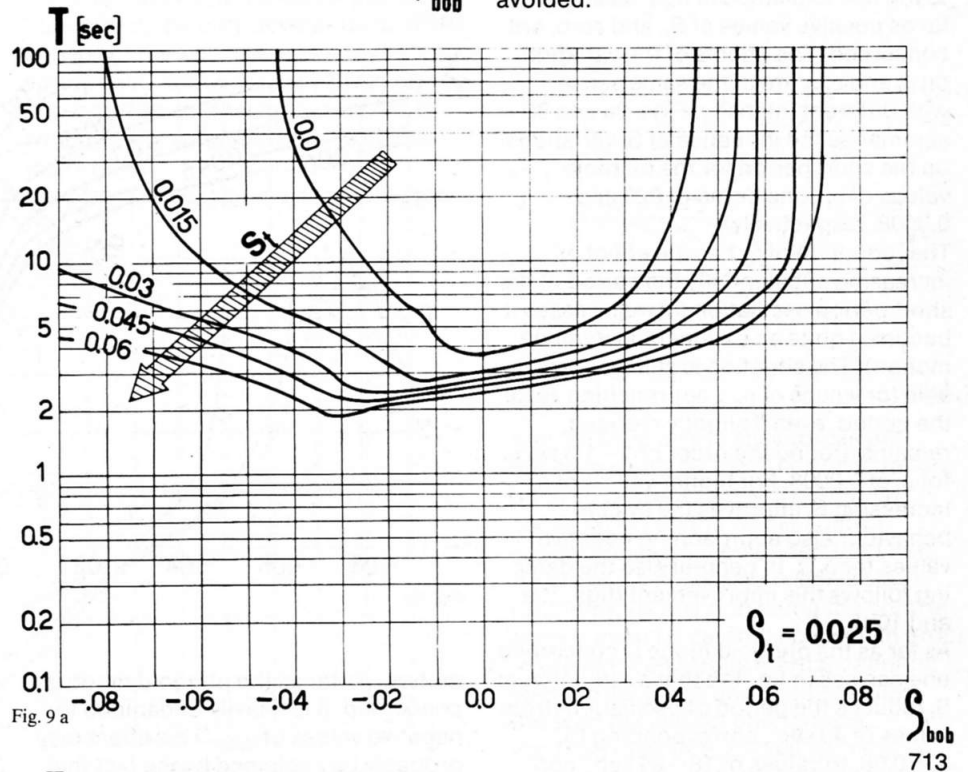


Fig. 9a

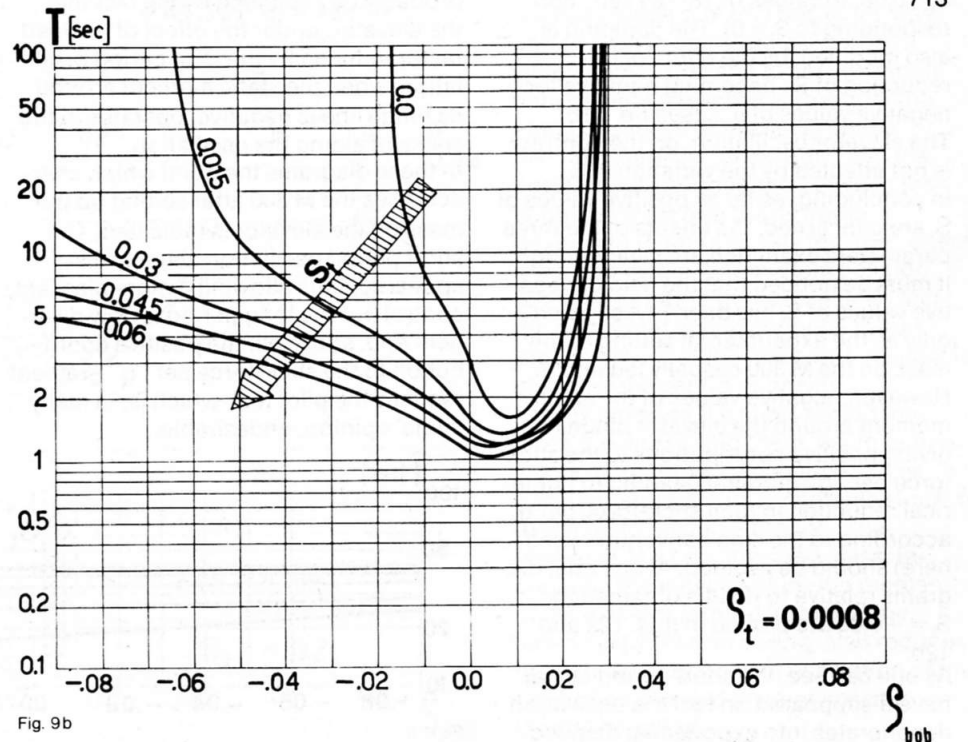


Fig. 9b

responding approximately to the intersections with the curves for the elevator oscillation ($Q_{bob} = -0.023, -0.01, 0.0$), for the usual three values of q_t . Probably, for these particular values of Q_{bob} , for which the short period damping approaches zero, a sort of resonance arises between sailplane short period mode and the elevator control-system oscillation.

In further increasing Q_{bob} the short period becomes undamped and then degenerates into exponential divergent motions. These indications can only be considered as qualitative, for one must remember the initial assumptions of small disturbances around the trimmed conditions. Nevertheless, the result is indicative of the fact that such values of Q_{bob} are to be avoided.

Referring still to figs. 8a and 8b, one can see that the points representing the situation of the M 300 before the correction by setting the mass on the control system are emphasised: the sailplane's free motion was characterised by an imperceptible long period slightly damped ($T=40$ secs., $\zeta=0.005$). On the contrary, as noticed by the pilot, the short period oscillation was quite undamped with a period of approximately 1.2 secs., resulting in a very unpleasant flight.

In continuing this analysis, several diagrams, like this one, were plotted, each for a different value of S_t , 0.045, 0.03, 0.015, 0.0, -0.015 , -0.03 , respectively. Without considering each of them, one can say that the situation remains similar to the one explained in figs. 8a and 8b as far as positive values of S_t , and zero, are concerned. The effects of the variation on Q_t and Q_{bob} are in the same sense, with different intensity. Figs. 9a and 9b summarise the influence of S_t variations on the short period for the extreme values of Q_t considered (0.025 and 0.0008, respectively).

The reduction of S_t has the effect of increasing substantially the period of the short period oscillation (in many cases it becomes quite an exponential damped motion). The situation is still unacceptable for values of Q_{bob} approaching zero: the period, even if slightly reduced, remains around the order of 1 – 1.5 secs. for Q_t of 0.0008. For higher values of Q_t , increasing S_t improves the system behaviour also approaching negative values for Q_{bob} . In general also the damping follows this improvement (figs. 10a and 10b).

As far as the phugoid mode is concerned, one can see in fig. 11a that a reduction of S_t reduces the period of oscillation (from values of 40 sec., corresponding to $S_t=0.06$, to values of 18 – 24 sec., corresponding to $S_t=0$). The damping is also modified, by the effect of the reduction of S_t , becoming negative for negative values of Q_{bob} (see fig. 11b). The elevator oscillation, on the contrary, is not affected by the variation in S_t . In concluding, as far as positive values of S_t are concerned, the effects of the three parameters examined are clear enough. It must be noticed that the field of negative values of S_t has been investigated only as the experimental setting of the mass on the M 300 casually led into it. However, negative values of the static moment around the elevator hinge line, giving positive contributions to the stick-force per "g" gradient (leading to numerical reduction in total stick-force per g, according to the sign convention used here) should be avoided. At any rate, diagrams relative to results obtained for $S_t = -0.03$ are plotted in figs. 12a and 12b.

As one can see, the short period curves have disappeared; in fact the oscillation degenerates into exponential damped

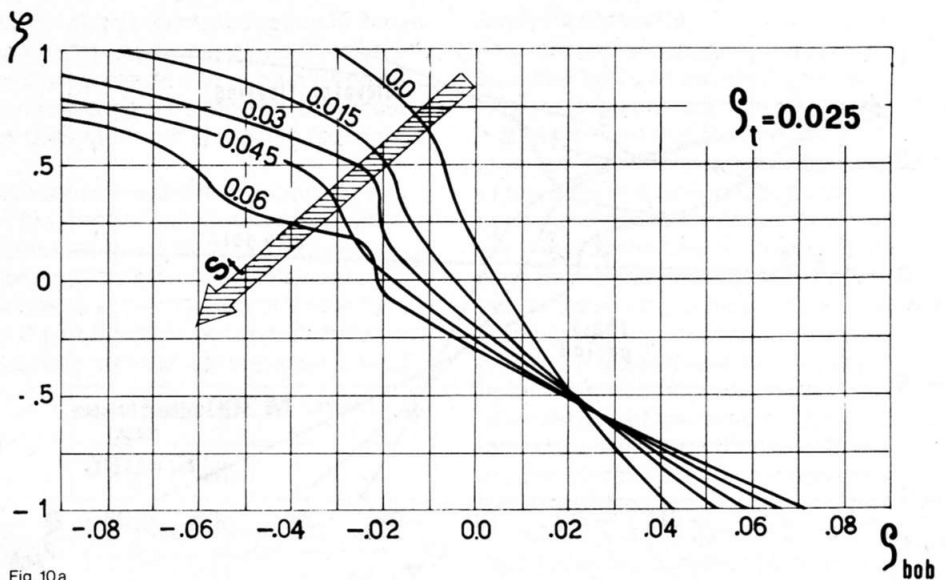


Fig. 10a

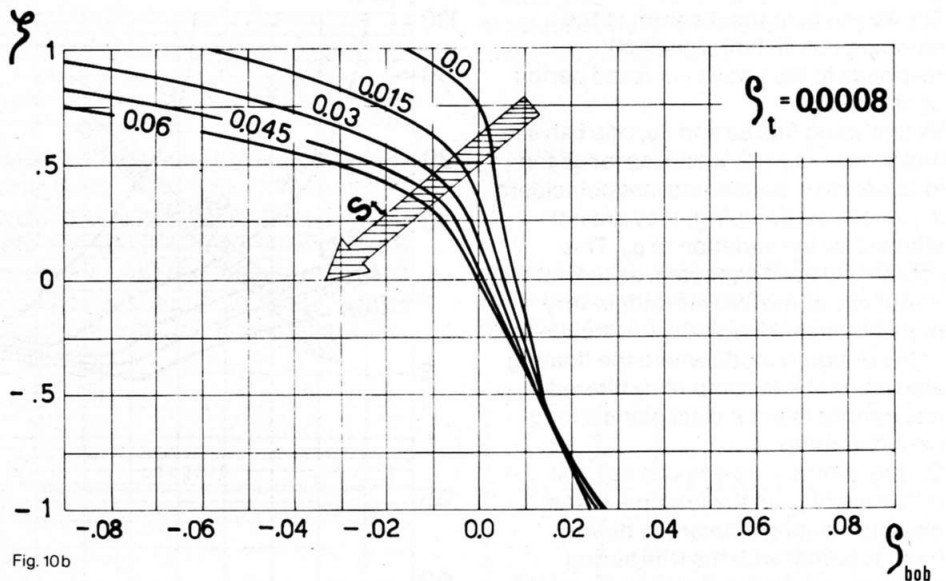


Fig. 10b

motion. As far as the phugoid mode is concerned, it is heavily undamped for negative values of Q_{bob} . This effect may probably be explained by the fact that the elevator, under the effect of the load factor induced by the long period oscillation, when the static moment around its hinge line is negative, operates in the sense of aiding the oscillation. In these diagrams the point which characterises the M 300 after setting up the mass on the elevator is indicated. The short period oscillation actually disappeared, thus allowing a more pleasant control but the long period is now divergent and, above all, the positive contribution to the stick-force per "g" gradient reduces the pilot feel, which is, in many pilots' opinion, undesirable.

After individualising possible sets of the parameters S_t , Q_t , Q_{bob} , which lead to a favourable dynamic behaviour of the sailplane stick-free, it is now possible to look for the best position of the mass (or masses) and for its (or their) best kinematical linkage. In fact, on the basis of the expressions:

$$[10] \quad m_i = \frac{\Delta S_{t_i}}{b_i K_i} \left[\frac{(Q/g) S_e l_e}{S} \right]$$

$$L_i = \frac{\Delta Q_{bob_i}}{\Delta S_{t_i}} \left[\frac{z \rho S}{Q/g} \right]$$

the mass which is to be set up and its distance from the center of gravity of the sailplane can be directly obtained (see figs. 13 and 14).

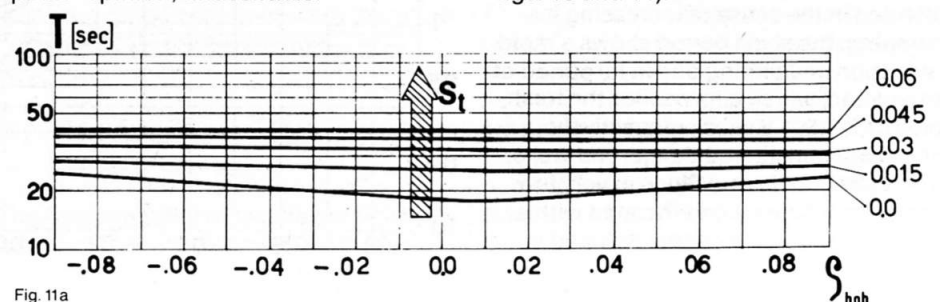


Fig. 11a

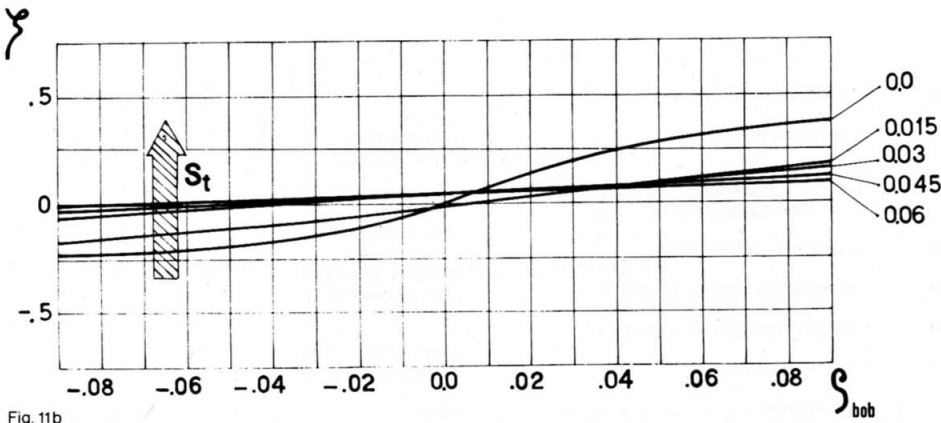


Fig. 11b

Concluding Remarks

The problem of the pilot induced oscillations (PIO) is a very complex one and is directly connected with the features of the closed loop pilot-sailplane. Although the problem is still open, it is general thought that the main factors are the short period characteristics and the stick-force per "g" gradients (ref. 4 and 7). Each of these two has its effect on pilot's response. Whilst on the civil and

military aircraft of today complex systems are adopted to give artificial feel to the pilot and, at the same time, to prevent PIO phenomena, as far as sailplanes are concerned, the only devices used, if any, consist of the bob-weights and the spring-feel. This is in order to satisfy the compromise cost-weight-complexity which, in the sailplane field, is of vital importance.

However, these systems, developed on

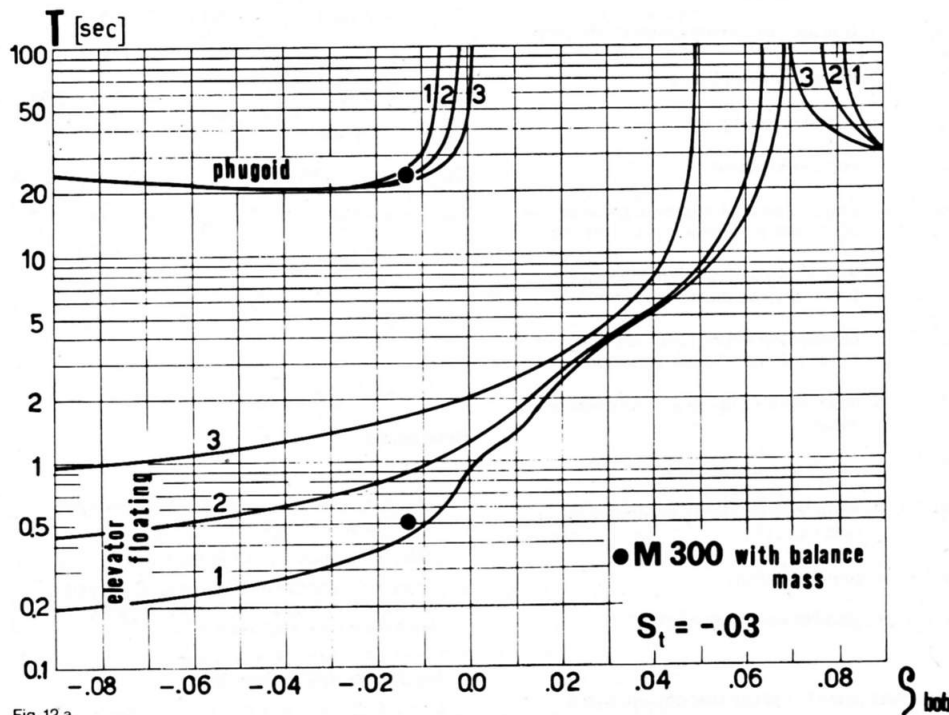


Fig. 12a

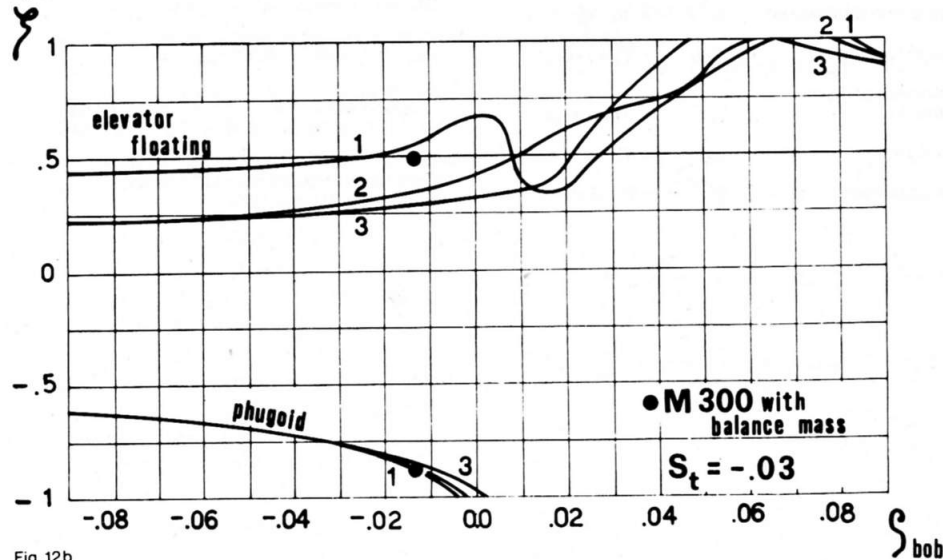


Fig. 12b

the basis of static considerations, are sometimes dangerous in dynamic maneuvering situations, where interaction between the control circuit and the airframe may produce control difficulties. In particular cases, if the pilot tries to interfere with the free sailplane oscillation,

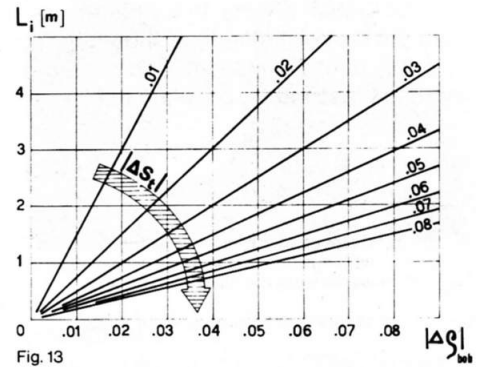


Fig. 13

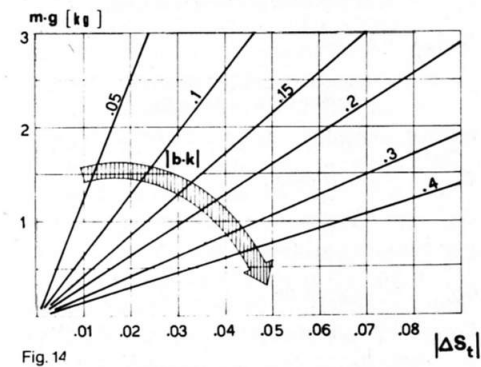


Fig. 14

tion, he feels on the stick forces produced not only by the C.G. acceleration, but also by the effect of the angular acceleration on the whole control system. One can then understand that, if a weight is necessary to solve static problems, its position along the control system must be carefully chosen in order to prevent dangerous inertial coupling with the sailplane and possible pilot-induced oscillation phenomena. Far from intending to deal with the complex subject of PIO this study was undertaken to investigate a problem which comes first and is not yet dependent on pilot's response: to clarify the effect of a mass (or masses) on the dynamic stability "stick-free" and the possible inertial coupling between the control system and the airframe. According to this analysis the main effect is caused by the longitudinal position of the mass along the sailplane; in fact the parameter which contains the distance $L = l + b$ of the mass with respect to the sailplane centre of gravity, Q_{bob} , heavily modifies the short period features, i. e. improving them, when reducing its magnitude for negative values; positive values are unacceptable since they lead to unstable motion. The presence of a concentrated mass, increasing the equivalent inertia moment of the elevator around its hinge line, aided by a light trim spring, also reduces the natural frequency of oscillation of the control-circuit and favours possible inertial coupling.

In concluding, the critical aspect of bob weights has been pointed out but, at this moment, the study is still at its first phase and many questions are still open. In particular the phase angles between the three modes of oscillation should be investigated in order to explain better the inter-action effects. In further investigations the pilot response should be introduced into the loop to find out more about the fascinating problem of PIO.

List of symbols

b_i	= distance of the balance weight "i" from its hinge line (measured positive backwards from the hinge, see fig. 4)
C_D	= sailplane drag coefficient = D/qS
$C_{D\alpha}$	= $\partial C_D / \partial \alpha$
C_L	= sailplane lift coefficient = L/qS
$C_{L\alpha}$	= $\partial C_L / \partial \alpha$
C_{MG}	= moment coefficient about the sailplane C. G. = $M_G/qS l_m$
$C_{M\alpha}$	= $\partial C_M / \partial \alpha$
$C_{M\alpha'}$	= $\partial C_M / (d\alpha/dt)$
$C_{M\delta}$	= $\partial C_M / \partial \delta$
$C_{M\delta'}$	= $\partial C_M / (d\delta/dt)$
$C_{M\dot{\theta}}$	= $\partial C_M / (d\dot{\theta}/dt)$
$C_{M\ddot{\theta}}$	= $\partial C_M / (d\ddot{\theta}/dt)$
C_μ	= general expression of the elevator hinge moment coefficient = $H/(qS_e l_e)$
$C_{\mu 0}$	= elevator zero lift moment coefficient
$C_{\mu\delta'}$	= $\partial C_\mu / \partial (d\delta/dt)$
$C_{\mu\dot{\theta}'}$	= $\partial C_\mu / \partial (d\dot{\theta}/dt)$
$C_{\mu\ddot{\theta}'}$	= $\partial C_\mu / \partial (d\ddot{\theta}/dt)$
C. G.	= sailplane centre of gravity
D	= sailplane drag
g	= acceleration due to gravity
G	= elevator gearing = $d\delta/ds$ where s = stick travel
H	= elevator hinge moment
i	= identification of a particular element of a series: $i = 1, 2, 3 \dots$
J_y	= sailplane inertia moment (With respect to the pitching y axis)
k_i	= mass gearing = $d\delta_i/d\delta$ where δ_i is the angular displacement of the balance weight "i" around its hinge line
k_{trim}	= spring stiffness (in the trimmed situation)
l_e	= elevator reference chord

l_i	= distance of the hinge "i" from the sailplane C. G. (measured positive backward; see fig. 4)
l_m	= wing mean aerodynamic chord
L	= sailplane lift
L_i	= $l_i + b_i$ = distance of the balance weight "i" from sailplane C. G.
m	= Q/g = sailplane mass
m_i	= mass of the balance weight "i"
M_G	= longitudinal (pitching) moment
n	= L/Q = load factor
P	= stick force
$\partial P / \partial n$	= stick-force per "g" gradient
q	= $\rho V_t^2 / 2$
Q	= sailplane weight
s	= stick travel
S	= sailplane wing area
S_e	= elevator area
t	= time
T	= period of oscillation
V	= true airspeed
V_t	= true airspeed in the trimmed situation
x	= longitudinal wind axis
y	= lateral (pitching) axis
z	= vertical wind axis
α	= angle of attack (measured between the flight path and the wing zero lift line)
γ	= $\dot{\theta} - \alpha$ = angle between the tangent to trajectory and the horizon line
δ	= elevator deflection angle with respect to the trimmed (reference) situation
Δ	= indicates a variation around a reference value
$\dot{\theta}$	= sailplane angle of pitch
λ	= complex root of stability equation (see expr. [7])
ρ	= air mass density
τ	= aerodynamic time = $t_0 S V_t / m$

Main data (used in the calculations within the text)

sailplane total weight	Q	= 305 kg
wing loading	Q/S	= 33.49 kg/m ²
moment of inertia about y	J_y	= 51 kg.s ² .m
wing span	b_w	= 15 m
wing surface	S	= 9.108 m ²

wing aspect ratio	A	= 24.51
wing lift curve slope	a_w	= 6.03 (per radian)
wing setting	i_w	= 4.5°
wing mean aerodynamic chord	l_m	= 0.621 m
wing aerodynamic centre location (as a fraction of l_m)	x_a/l_m	= 0.25
sailplane centre of gravity location (as a fraction of l_m)	x_G/l_m	= 0.41 $z_G/l_m = 0.5$
wing section lift curve slope (Eppler 266)	a_O	= 6.14 (per radian)
tail arm	l_t	= 3.76 m
tail surface	S_e	= 0.72 m ²
tail mean aerodynamic chord	l_e	= 0.27 m
elevator gearing	G	= 3.15 m ⁻¹
acceleration due to gravity	g	= 9.81 m/s ²
flight altitude	z	= 1000 m

Coefficients of the stability determinant (in the reference situation):

C_D	= 0.02215	$C_{M\delta}$	= -2.492
$C_{D\alpha}$	= 0.1629	$C_{M\delta'}$	= -0.0273
C_L	= 0.8	S_t	= -0.03 ÷ 0.06
$C_{L\alpha}$	= 6.39	e_{bob}	= -0.09 ÷ 0.09
$C_{M\alpha}$	= -1.344	$C_{\mu\dot{\theta}}$	≅ 0
$C_{M\alpha'}$	= -0.04365	e_t	= 0.0008 ÷ 0.025
$C_{M\dot{\theta}}$	= -0.343	$C_{\mu\delta}$	= -0.015
h	= 0.1755	K	= 0.09945

References

- Perkins, C. D. and Hage, R. E., «Airplane Performance, Stability and Control», Wiley.
- Etkin, B., «Dynamics of Flight», Wiley.
- Jones, R. T. and Cohen, D., «An Analysis of the Stability of an Airplane with Free Controls», NACA Report nr. 709, 1941.
- Morelli, P., «Static Stability and Control of Sailplanes», OSTIV, May 1976.
- Irving, F. G., «PIO's in glider», «Sailplanes and Gliding», February-March 1969.
- Irving, F. G., «All moving Tailplanes», «OSTIV Publication VII», (1963 Argentina).
- Sandauer, J., «Dynamic Characteristic of a sailplane with all-moving Tail», from the paper nr. 47 of the Prace Instytutu Lotnictwa, 1971.
- Gibson, J. C., «Some Notes on Handling Qualities», «Sailplanes and Gliding», August-September 1969.